

Temporal Credit Is Free

Aur Shalev Merin

March 2026

Abstract

Recurrent networks do not need Jacobian propagation to adapt online. The hidden state already carries temporal credit through the forward pass; immediate derivatives suffice if you stop corrupting them with stale trace memory and normalize gradient scales across parameter groups. An architectural rule predicts when normalization is needed: β_2 is required when gradients must pass through a nonlinear state update with no output bypass, and unnecessary otherwise. Across ten architectures, real primate neural data, and streaming ML benchmarks, immediate derivatives with RMSprop match or exceed full RTRL, scaling to $n = 1024$ at $1000\times$ less memory.

1 Introduction

Training recurrent networks online means assigning credit across timesteps: how did past inputs affect the current error? The standard answer, real-time recurrent learning [Williams and Zipser, 1989], propagates a Jacobian tensor forward through the network’s dynamics at $O(n^4)$ cost per step. Thirty years of work since then has tried to make this cheaper. Every approach assumes the Jacobian term carries gradient information you cannot get any other way. We revisit that assumption.

It is not needed. The hidden state already carries temporal credit through the forward pass. The immediate derivative, computed through that state, is enough for online adaptation. Eligibility traces fail for two reasons: the standard decay rate (0.95) overweights stale gradients by $85\times$ relative to the true propagation factor, and without per-parameter normalization, recurrent weight updates get drowned out by output gradients that are $100\times$ larger. Adam’s β_2 partially compensates for bad decay (18% recovery vs 0% for SGD), but full adaptation requires both corrections (Table 1).

We make four claims, each tested independently:

- Eligibility traces fail because of two miscalibrations, not because they lack the Jacobian. The standard decay (0.95) overweights stale gradients by $85\times$ relative to the measured self-propagation factor, and uniform learning rates cannot bridge the $100\times$ gradient scale gap between recurrent and output parameters.

Table 1: Recovery (%) on sine frequency-shift task ($n = 64$, 5 seeds). Recovery is defined as $(M_{\text{frozen}} - M_{\text{post}})/(M_{\text{frozen}} - M_{\text{RTRL}})$, where M is post-shift MSE; values above 100% mean the method outperforms full RTRL. Two factors interact: trace decay and optimizer. Adam partially compensates for bad decay (18%) but full adaptation requires both corrections.

	SGD	Adam
$\lambda = 0.95$ (standard)	0%	18%
$\lambda = 0.0$ (ours)	-1%	102%

- Correcting both (zero decay, β_2 normalization) recovers full RTRL performance without any Jacobian computation. On chaotic dynamics and real BCI data, it beats full RTRL in both accuracy and stability.
- An architectural rule predicts when β_2 is needed: it is necessary when adaptation must flow through a nonlinear or multiplicative state update, and unnecessary when the architecture provides a parallel output path. The rule holds across nine architectures (Table 3) plus a tenth (LeWM transformer) evaluated via gradient diagnostics.
- The method scales to $n = 1024$ at $1000\times$ less memory than RTRL (12.6 MB vs 12.9 GB). Online LoRA adaptation with β_2 achieves 21–134% recovery on five pretrained language models from 124M to 7B parameters, single-pass, no replay. Rank-16 adapters reach 136.8% recovery. SGD with identical adapter capacity shows zero adaptation everywhere.

2 Background

Online learning in recurrent networks requires computing the gradient of a streaming loss with respect to model parameters at each timestep. Real-time recurrent learning [Williams and Zipser, 1989] does this by maintaining a sensitivity tensor $P_t = \partial h_t / \partial \theta$, updated recursively as

$$P_t = J_t P_{t-1} + \left. \frac{\partial h_t}{\partial \theta} \right|_{\text{direct}}, \quad (1)$$

where $J_t = \partial h_t / \partial h_{t-1}$ is the state Jacobian. The $J_t P_{t-1}$ term propagates credit from past timesteps. Computing it costs $O(n^4)$ per step for a network with n hidden units, which has limited RTRL to small networks and motivated thirty years of approximation methods.

Eligibility traces [Murray, 2019, Bellec et al., 2020] avoid this cost by replacing J_t with a scalar or diagonal approximation:

$$e_t = \lambda e_{t-1} + \left. \frac{\partial h_t}{\partial \theta} \right|_{\text{direct}}. \quad (2)$$

The decay λ (typically 0.95) is meant to approximate the fading influence of past timesteps. This reduces cost to $O(n^2)$ but discards most of the recurrent component of the gradient. The resulting traces are biologically motivated and computationally cheap, but they fail to adapt to distribution shifts in practice, a failure typically attributed to the missing Jacobian term.

Adam [Kingma and Ba, 2015] maintains a per-parameter running estimate of squared gradient magnitudes: $v_t = \beta_2 v_{t-1} + (1 - \beta_2) g_t^2$. Each parameter update is then normalized by $\sqrt{v_t}$, which equalizes effective learning rates across parameters with different gradient scales. In standard usage this is a training convenience. In recurrent networks, where nonlinear activations compress recurrent gradients to be orders of magnitude smaller than output gradients, this normalization has a more specific role that we identify in Section 4.

2.1 Related work

Since Williams and Zipser [1989], online recurrent learning has focused on computing or approximating the Jacobian product $J_t P_{t-1}$: exact methods at $O(n^4)$ [Williams and Zipser, 1989], rank-1 compression at $O(n^2)$ [Tallec and Ollivier, 2017], optimal Kronecker-sum approximation at $O(n^3)$ [Benzing et al., 2019], graph-structured sparsity for weight-sparse networks [Menick et al., 2021], diagonal recurrence exploited for efficiency [Zucchet et al., 2023], and architectural elimination of inter-neuron recurrence [Irie et al., 2024]. Marschall et al. [2020] provide a unified taxonomy. These methods span four orders of magnitude in cost but share an assumption: the $J_t P_{t-1}$ term carries gradient information that cannot be recovered from the immediate derivative alone.

Murray [2019] and Bellec et al. [2020] took a different approach, dropping J_t and retaining only immediate derivatives with a scalar or diagonal decay. This is equivalent to our decay > 0 baseline. Their methods are neurally plausible and cheap, but neither identified the two factors that make immediate derivatives sufficient: Murray uses $\lambda = 0.9$, which overweights stale gradients relative to the true propagation factor, and neither method uses per-parameter gradient normalization. With these corrections (decay = 0, β_2), the approach they pioneered matches or exceeds full RTRL.

Per-parameter adaptive learning rates [Kingma and Ba, 2015] are well understood for batch training. Their role in online recurrent learning has not been examined. We show that second-moment normalization is not a training convenience in this setting but a necessary correction for a specific architectural problem: the gradient scale mismatch that nonlinear recurrences create between parameter groups. This connection between optimizer design and online recurrent adaptation is, to our knowledge, new. Concurrent work on test-time training [Sun et al., 2024, Akyürek et al., 2026] adapts model weights during inference via gradient updates, achieving context compression and long-sequence efficiency. These methods use Adam but do not examine why per-parameter normalization is necessary. Our findings explain why: without β_2 , the gradient scale mismatch between parameter groups prevents adaptation (SGD achieves 0% recovery across all configurations tested).

3 The trace decay mismatch

The standard explanation for why eligibility traces fail is that they discard the Jacobian term $J_t P_{t-1}$, losing the recurrent component of the gradient. We propose a simpler explanation: the trace decay is miscalibrated.

The starting point was an accident. In prior work on sparse Jacobian transport [Shalev Merin, 2026], a sweep over sparsity levels found that propagating a single random Jacobian column ($k = 1$) recovers 86% of full RTRL performance at $n = 64$. Due to the ring mask implementation, $k = 1$ produces an empty propagation mask, meaning it computes only the immediate derivative with zero Jacobian propagation. If zero temporal propagation recovers most of the signal, why do standard eligibility traces, which also lack full Jacobian propagation, fail?

In a trained vanilla RNN with hidden size 64, we measured the per-neuron self-propagation factor: $\text{diag}(1-h_t^2) \cdot \text{diag}(W_{hh})$, averaged over timesteps. This is the rate at which each neuron’s own past value influences its present through its recurrent self-connection. The measured value is approximately 0.01 per step. (The spectral radius of the full Jacobian $D_t W_{hh}$ is higher, typically 0.37–0.93, because cross-neuron interactions contribute additional propagation. But scalar trace decay is a per-neuron approximation: it applies one λ to each neuron’s trace independently, without modeling cross-neuron coupling. The diagonal, not the spectral radius, is the right quantity to compare it against.) With $\lambda = 0.95$, information from 10 steps ago is weighted at $0.95^{10} \approx 0.60$ by the trace, while its true per-neuron influence is $0.01^{10} \approx 10^{-20}$. The per-step overweighting is $85 \times (0.95/0.01)$, and the cumulative gap grows exponentially with horizon.

This is not a subtle discrepancy. At timestep 500 in a trained network, the accumulated trace ($\lambda = 0.95$) is 6.7 times larger in magnitude than the immediate derivative and points in a different direction (cosine similarity 0.577). The trace does not provide useful temporal credit. It provides stale gradient information at wildly incorrect scale. The immediate derivative, computed through h_{t-1} which already encodes the full history of inputs through the forward pass, is both more accurate and more relevant.

Figure 1 shows the consequence. We sweep trace decay from 0.001 to 0.95 on a sine frequency-shift task at two scales ($n = 64$, $n = 256$, five seeds each), all with Adam ($\beta_1 = 0.9$, $\beta_2 = 0.999$). At both scales, decay values from 0.001 to 0.5 produce successful adaptation (102–130% recovery at $n = 64$, 163–200% at $n = 256$). Recovery exceeding 100% indicates the adapted model outperforms the full RTRL reference on the target distribution, which occurs when full RTRL is itself unstable or when the simpler gradient acts as implicit regularization. Decay 0.95 produces exactly 0% recovery on every seed at every scale. The transition between working and failing is sharp: decay 0.7 shows high variance ($77 \pm 56\%$ at $n = 64$), indicating seed-dependent threshold behavior, while decay 0.5 works reliably ($130 \pm 8\%$). The entire region below 0.5 is a safe plateau; the standard default of 0.95 sits on the wrong side of a cliff.

The optimal decay value is not zero everywhere. At $n = 64$, decay 0.5 outperforms decay 0.001 by 28 percentage points (130% vs 102%), likely due

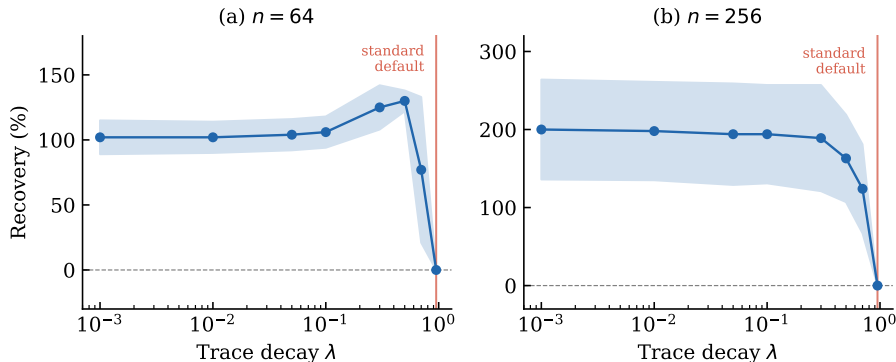


Figure 1: Recovery vs. trace decay on a sine frequency-shift task (5 seeds, mean ± 1 std). The standard default ($\lambda = 0.95$) produces 0% recovery at both scales. Values below 0.5 form a safe plateau. The optimal decay decreases with network size: at $n = 256$, all values ≤ 0.5 are statistically indistinguishable.

to a mild regularization effect from residual trace memory. At $n = 256$, this advantage disappears: error bars overlap across the entire $d \leq 0.5$ range. The optimal decay decreases with network size, and at scales that matter for practice ($n = 256$ and above), zero is indistinguishable from any other value in the safe range. We recommend zero as the default because it requires no tuning and works at every scale tested. Its interpretation is direct: use the immediate derivative and let the hidden state carry temporal information through the forward pass.

The pattern holds on real data. On cross-session BCI data from primate reaching experiments, using Adam, decay 0.0 achieves 74% recovery, decay 0.5 achieves 82%, and decay 0.95 achieves 46%. On BCI data, small nonzero decay provides a marginal benefit (82% vs 74%), consistent with slower neural dynamics where short-term trace memory is helpful at 50 ms time bins. Zero decay still passes the adaptation threshold on all seeds. On a character-level language task (Shakespeare to Python domain shift), decay 0.0 matches BPTT to three decimal places (cross-entropy 2.716 vs 2.718). On chaotic dynamics (Lorenz attractor), decay 0.0 recovers 113% while decay 0.95 recovers 0%. The pattern is consistent: low or zero decay works, the standard value fails.

4 The role of gradient normalization

Correcting the trace decay is necessary but not sufficient. With decay set to zero, SGD recovers -1% (Table 1), no better than a frozen model. The immediate derivative is now correct in direction, but SGD cannot use it. The problem is gradient scale.

In a trained vanilla RNN ($n = 64$), we measured the mean gradient norm for

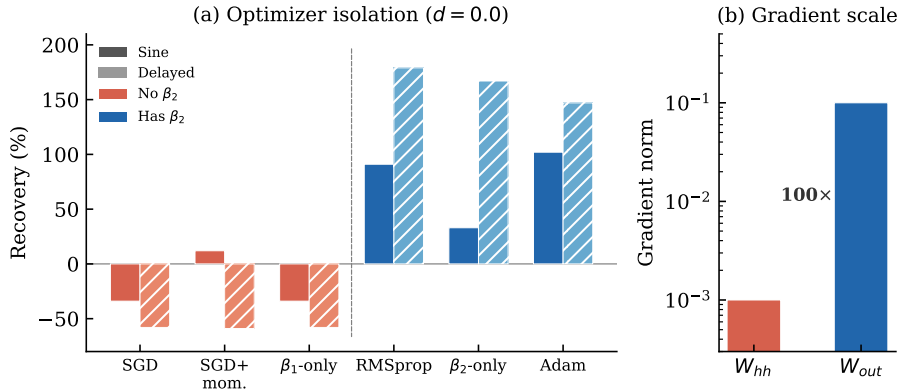


Figure 2: (a) Optimizer isolation with immediate derivatives ($\lambda = 0$). Only methods with second-moment normalization (β_2) adapt. Momentum (β_1) adds nothing. (b) Gradient norms by parameter group in a trained vanilla RNN ($n = 64$), showing the $100\times$ scale mismatch between recurrent and output weights.

Table 2: Optimizer isolation: recovery (%) with immediate derivatives ($\lambda = 0$). Only methods with β_2 adapt; momentum alone adds nothing.

Optimizer	Sine	Delayed ($t+50$)
SGD	-34	-58
SGD + momentum	12	-59
Adam β_1 -only	-34	-58
RMSprop ($\alpha = 0.99$)	91	179
Adam β_2 -only	33	167
Adam (full)	102	147

each parameter group during online adaptation. The recurrent weight gradients ($\partial L / \partial W_{hh}$) are approximately 100 times smaller than the output weight gradients ($\partial L / \partial W_{out}$). This is a direct consequence of the activation function: the tanh derivative ($1 - h_t^2$) compresses gradients flowing through the recurrence, while the output path is a direct linear projection with no compression. SGD applies the same learning rate to both groups, so recurrent weight updates are 100 times smaller in effective magnitude than output updates. The network adapts its output mapping but cannot adjust its dynamics.

Table 2 isolates the mechanism using BPTT with a window of one step. This computes the same immediate derivative as $\lambda = 0$ traces but through PyTorch autograd, which includes gradient clipping and the full single-step computation graph. The difference is substantial: with autograd, SGD learns pre-shift (MSE ≈ 0.03) but fails to adapt (-34%), while with manual traces SGD never learns

at all (pre-shift MSE ≈ 0.5 , recovery -1% in Table 1). The autograd results are more informative because they isolate the adaptation failure from the training failure. We trained vanilla RNNs under six optimizer configurations so that the only variable is the optimizer. The pattern is unambiguous. Every configuration with second-moment normalization (β_2) adapts. Every configuration without it fails. Momentum (β_1) averages gradient direction over time, which is the closest thing to temporal credit assignment that an optimizer provides. It adds nothing: β_1 -only recovery (-34%) is identical to raw SGD (-34%). The mechanism is per-parameter scale normalization, not temporal averaging of any kind. RMSprop ($\alpha = 0.99$) outperforms full Adam on the delayed task (179% vs 147%), confirming that β_2 alone, without momentum or bias correction, is the active component. The Adam-to-SGD control (switching optimizer at the shift with a pre-trained model) confirms this is about adaptation, not training: SGD achieves only 6% recovery with a fully converged model, while Adam achieves 100% and β_2 -only achieves 93%. With miscalibrated decay ($\lambda = 0.95$), even Adam achieves only 18% recovery: β_2 partially compensates for stale traces but cannot fully overcome them.

A possible objection is that β_2 's running second moment ($v_t = \beta_2 v_{t-1} + (1 - \beta_2)g_t^2$, with an effective window of ~ 1000 steps at $\beta_2 = 0.999$) is itself a form of temporal credit propagation through a different channel. We can test this directly. We trained a model to convergence with Adam, then switched the optimizer to SGD at the distribution shift, keeping all model parameters identical. If the trained model's gradient quality is sufficient and only the optimizer matters at adaptation time, SGD should work with a converged model even if it cannot train from scratch. It does not: recovery is 6%. The same switch to Adam yields 100%, and to β_2 -only yields 93%.

The mismatch is not about what the model learned during training. It is about what the optimizer does at each adaptation step: normalizing $g_t/\sqrt{v_t}$ equalizes effective learning rates across parameter groups with different gradient scales. This is scale calibration, not credit assignment.

The gradient scale mismatch in vanilla RNNs arises specifically from tanh compression. Any nonlinear activation that differentially compresses gradients through the state update should produce a similar mismatch. We test this prediction across architectures in the next section.

5 Cross-architecture generalization

The trace decay and gradient scale findings were established on vanilla RNNs. If the underlying cause is architectural (nonlinear activations compressing recurrent gradients), the same pattern should appear in any architecture with nonlinear state updates and disappear in architectures that provide an alternative adaptation path. We tested this across ten architectures. Table 3 summarizes the results.

The architectural rule can be stated precisely: per-parameter gradient normalization is necessary for online adaptation when two conditions hold simulta-

Table 3: Cross-architecture β_2 requirement on sine frequency-shift task (5 seeds unless noted, BPTT $w=1$ gradients; see Section 4 for comparison with manual traces). Architectures without an output bypass show large Adam/SGD gaps; architectures with a bypass show no gap or inverted behavior. [‡]RWKV shows inverted behavior on Lorenz: all β_2 -containing optimizers diverge, only SGD survives (see text).

Architecture	Adam/ β_2	SGD	Grad. ratio	Bypass
Vanilla RNN	102%	-34%	100×	None
LSTM	99.7%	59.4%	~31×	None
CTRNN	89.8%	-0.1% (=frozen)	278×	None
xLSTM (sLSTM)	91.5%	60.0%	~24×	None
RWKV [‡]	adapts	0% (=frozen)	∞ (zero rec.)	None
RetNet	93%	-17%	~64×	None
Vanilla GRU	adapts	adapts	5–19×	Update gate
SSM (S4)	adapts	adapts	<6×	C/D output
Block-GRU+MLP	adapts	50× better	50000×	MLP output

neously. First, the recurrent state update involves a nonlinear or multiplicative transformation that compresses gradients. Second, there is no parallel output path with sufficient capacity for the model to adapt without updating the compressed recurrence. When either condition is absent, SGD suffices.

Six architectures confirm the rule on stable tasks (sine frequency-shift). Vanilla RNN, LSTM, CTRNN, xLSTM, RWKV, and RetNet all have nonlinear or multiplicative state updates and no parallel output path. In each case, SGD either fails entirely or performs dramatically worse than Adam, and gradient norm measurements confirm the same pattern: recurrent parameter gradients are 100× to 50,000× smaller than output parameter gradients. The compression source varies across architectures (tanh saturation in RNNs and CTRNNs, sigmoid gating in LSTMs and xLSTM, multiplicative key-value interaction in RWKV and RetNet), but the consequence is the same. β_2 normalizes the mismatch. SGD cannot.

On chaotic dynamics (Lorenz), the rule holds for most architectures but two show task-dependent behavior. xLSTM’s exponential gating allows SGD to adapt on Lorenz (100% recovery, 5 seeds) despite failing on sine (60%, 24× worse than RMSprop). RWKV exhibits an inversion: on Lorenz, all three β_2 -containing optimizers (Adam β_2 -only, full Adam, RMSprop) diverge on every seed, while SGD is the only optimizer that survives (293% recovery, zero variance). Gradient norms explain the mechanism: under SGD, RWKV’s recurrent gradients are literally zero, so SGD effectively freezes the recurrence and adapts only through the output predictor, which has sufficient capacity for the Lorenz task. When β_2 normalizes these near-zero recurrent gradients, it amplifies them through the multiplicative $k \cdot v$ interaction, creating unstable updates on chaotic dynamics. The architectural rule correctly predicts the β_2 requirement on sta-

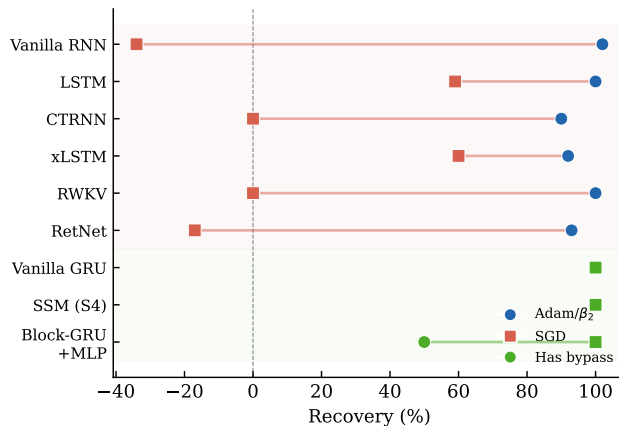


Figure 3: Adam/ β_2 (circles) vs. SGD (squares) recovery across ten architectures. Red background: no output bypass (β_2 required). Green background: has output bypass (SGD suffices or is better). The gap between dots is the β_2 requirement.

ble tasks; on chaotic dynamics, multiplicative state updates can make gradient normalization destabilizing.

Standard LSTM is worth examining separately because its cell state provides a gradient highway for backpropagation through time, which is the classic mechanism for avoiding vanishing gradients. One might expect this highway to also bypass the gradient scale mismatch. It does not. The sigmoid gates (input, forget, output) still compress recurrent gradients, producing a $31\times$ mismatch between recurrent and output parameter norms. SGD recovery is 59% on sine and 8% on Lorenz (5 seeds, near-zero variance). The cell state helps with long-range credit in BPTT but does not help with gradient scale normalization in online adaptation. Gated recurrences compress gradients regardless of internal memory structure.

RetNet has a linear decay built into its recurrence, which looks like it should provide a gradient path that avoids nonlinear compression. It does not help. The key-value outer product in RetNet’s state update compresses recurrent gradients regardless of the linear decay factor. On Lorenz, SGD recovery is -17% : not just failing but actively harmful, producing worse performance than a frozen model. The linear decay preserves state magnitude but does not preserve gradient magnitude through the multiplicative interaction.

Three architectures break the pattern. Vanilla GRUs adapt under all optimizers, including SGD. The update gate $z_t = \sigma(W_z x_t + U_z h_{t-1})$ creates a linear interpolation $h_t = (1 - z_t) \odot h_{t-1} + z_t \odot \tilde{h}_t$ that provides a gradient path bypassing the nonlinear candidate computation. The gradient ratio is $5\text{--}19\times$, small enough for SGD to handle.

State space models (S4 variant, trained from scratch) adapt under all opti-

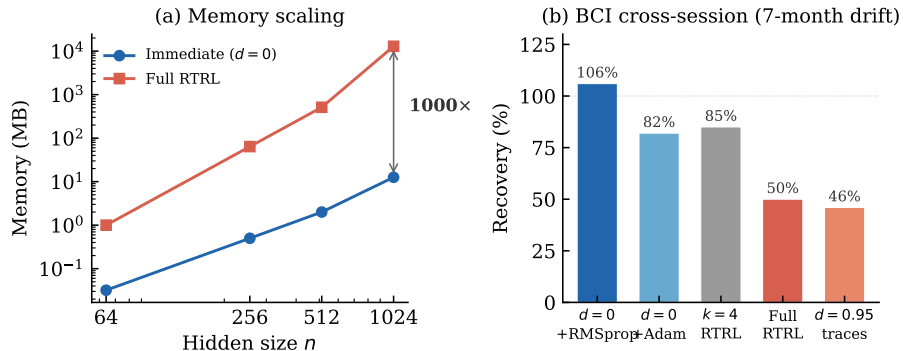


Figure 4: (a) Memory scaling: immediate derivatives ($d=0$) vs. full RTRL. At $n = 1024$ the gap is 1000 \times (12.6 MB vs. 12.9 GB). (b) Cross-session BCI decoding (7-month electrode drift, 5 seeds). $d=0$ + RMSprop (106%) exceeds all Jacobian-based methods.

mizers, including SGD. The reason is architectural: SSMS have a direct output path through the C and D matrices that bypasses the recurrent state update (A , B) entirely. Gradient norms confirm this. Recurrent parameter gradients are near zero, but the model does not need to update them. Adaptation happens through the output matrices, whose gradients are large and direct. The block-diagonal GRU architecture used in DreamerV3 [Hafner et al., 2024] shows a similar bypass through a different mechanism. A two-layer MLP with SiLU activation sits between the GRU output and the prediction, providing enough capacity for the model to learn a new output mapping from unchanged GRU states. On Lorenz, SGD outperforms Adam by 50 \times . The MLP output path provides direct, well-scaled gradients that do not benefit from per-parameter normalization; both momentum and second-moment normalization degrade performance on this architecture. The MLP receives 50,000 times more gradient than the GRU internals.

We also measured gradient uniformity in a pretrained transformer world model (LeWM; Maes et al. [2026]), a six-layer transformer with 16 attention heads and AdaLN conditioning. Within the predictor layers, gradient norms vary by less than 6 \times across layers, even through 20 autoregressive rollout steps. Residual connections prevent the differential compression that makes β_2 necessary in recurrent architectures. This confirms that the β_2 requirement is specific to architectures where gradients must pass through nonlinear state updates with no bypass.

6 Scaling and real-world validation

Table 4 summarizes the method comparison across all tested domains. Immediate derivatives with Adam or RMSprop match or exceed Jacobian-based

Table 4: Head-to-head comparison: immediate derivatives ($d=0$) vs. Jacobian-based methods across domains. All values are recovery (%) unless noted. “-” indicates not tested in that configuration. †Language row reports cross-entropy (lower is better); both methods match to three decimal places.

Domain	$d=0$ + Adam	$d=0$ + RMSprop	$k=4$ RTRL	Full RTRL
Sine ($n=64$)	102	73	125	100
Delayed ($t+50$)	147	179	130	100
Lorenz (chaotic)	113	-	-	100
BCI (real data)	82	106	85	50
Language (CE \downarrow) [†]	2.716	-	2.708	-
$n=1024$	378	-	-	can’t run

methods on every task, at $O(n^2)$ cost instead of $O(n^3)$ or $O(n^4)$.

The mechanism was established on small networks and synthetic tasks. Four questions follow: does it scale, does it work on real data, can it compete with existing methods, and does it extend to pretrained models?

Scaling. With decay set to zero, the method stores only the immediate derivative per parameter, requiring $O(n^2)$ memory. Full RTRL maintains the Jacobian sensitivity tensor at $O(n^3)$, and sparse RTRL ($k = 4$) reduces the constant but not the scaling. At $n = 64$, the difference is modest (32 KB vs 1 MB). At $n = 1024$, immediate derivatives require 12.6 MB while full RTRL requires 12.9 GB and cannot run on a single GPU. The ratio is 1000 \times . Recovery at $n = 1024$ is $378 \pm 76\%$ (five seeds), where the high recovery percentage reflects the full RTRL reference being unstable at this scale; absolute post-shift MSE is more informative and shows consistent adaptation across all seeds. Decay 0.95 at $n = 1024$ produces 0.54 MSE uniformly across seeds, indistinguishable from a frozen model.

Real neural data. We tested cross-session BCI decoding using primate reaching data [O’Doherty et al., 2017], with seven months of real electrode drift between sessions. Ninety-six electrode channels were reduced to 40 PCA dimensions fit on the source session only. Switching from Adam (82% recovery in Section 3) to RMSprop ($\alpha = 0.99$) improves recovery to $106 \pm 18\%$ across five seeds, with the adapted decoder performing comparably to or exceeding the original decoder on its own session. All five seeds exceed 84%. For comparison, sparse RTRL ($k = 4$) achieves 85% and full RTRL achieves only 50%, with two of five seeds partially diverging. RMSprop outperforms Adam on this task (106% vs 82%), consistent with its shorter effective memory window (~ 100 steps at $\alpha = 0.99$ vs ~ 1000 steps at $\beta_2 = 0.999$) being better suited to the timescale of neural drift at 50 ms bins.

Table 5: Online LoRA adaptation across pretrained LMs (rank-4 adapters, code-to-Wikipedia shift). Adam β_2 adapts at every scale; SGD shows zero adaptation regardless of model size or architecture.

Model	Params	Adam β_2	SGD
GPT-2	124M	21.6%	0.0%
Mamba-130M	130M	51.6%	0.1%
TinyLlama	1.1B	31.6%	0.1%
Mamba-1.4B	1.4B	133.5%	2.4%
Qwen2	7B	$31.3 \pm 7.3\%$	$0.0 \pm 0.4\%$

Streaming ML benchmarks. Online RNNs with decay 0.0 and Adam can outperform tree-based streaming methods on tasks dominated by continuous drift. On a head-to-head comparison using the Hyperplane generator from the River library [Montiel et al., 2021] with parameters matching Gomes et al. [2017] (200K samples, 10 features, gradual drift), the RNN achieves 0.925 accuracy versus Adaptive Random Forest at 0.842 (+8.3 pp). Tree ensembles retain their advantage on tasks requiring spatial partitioning (RandomRBF) and real-world tabular data (Electricity), where gradient-based adaptation cannot compensate for trees’ structural inductive bias.

Pretrained language models. The same β_2 requirement appears in pretrained models through LoRA adapters. We adapted five pretrained LMs online on domain shifts using LoRA adapters with single-pass processing and no replay. Table 5 shows the results across a $56\times$ scale range.

From 124M to 7B, SGD achieves zero adaptation across all models, adapter sizes, and learning rates tested. Adam β_2 achieves 21–134% recovery at rank-4; with rank-16 adapters and 40K tokens, GPT-2 recovery reaches 136.8% (cross-entropy 2.744, down from 3.493 frozen). Unlike the from-scratch architectures in Section 5, the β_2 requirement here arises from depth-induced gradient attenuation through the frozen backbone rather than nonlinear activation compression. Direct measurement of LoRA gradient norms on Mamba confirms this: across 24 layers and 3 matrix types, the gradient magnitude ratio between the largest group (L23 dt_proj, norm 1.35) and smallest (L15 x_proj, norm 0.026) is $51.8\times$. Last-layer gradients are $12\times$ larger than mid-network gradients, consistent with depth attenuation. The pattern spans both SSM-based (Mamba) and transformer-based (GPT-2, TinyLlama, Qwen2) architectures, confirming that depth attenuation, not any particular architecture, drives the mismatch.

To test whether online LoRA adaptation handles multiple sequential domain shifts, we streamed Code→Wiki→Code→Wiki through GPT-2 with a rank-4 adapter. Adam β_2 adapts to every shift (39% and 26% recovery on successive Wiki segments) while SGD shows zero adaptation across all four segments. The adapter does not forget: Code B cross-entropy (1.608) is lower than Code A (1.796), indicating the adapter improves on return to a previously seen domain.

Wiki readaptation is faster on second exposure (shock cross-entropy 2.612 vs 3.048), and the lower recovery percentage on Wiki B (26% vs 39%) reflects a smaller gap to close, not worse adaptation. No replay buffer, no task boundaries, single-pass.

Test-time adaptation in vision. The β_2 requirement depends on which parameters are adapted, not just whether adaptation happens. On CIFAR-10-C test-time adaptation (WideResNet-28-10, 15 corruption types at severity 5, 3 seeds), adapting only batch normalization affine parameters via entropy minimization [Wang et al., 2021] shows a 2.6 percentage point gap between Adam and SGD. BN parameters are the same type at every layer, so gradient scales are roughly uniform and β_2 adds little. Replacing BN with LoRA adapters at every convolutional layer widens the Adam–SGD gap to 7.6 pp (51.1% vs 43.5% recovery). β_2 -only matches Adam (52.3%), and β_1 -only falls between (46.0%). LoRA gradients span 28 layers with a 5–6 \times norm ratio between shallowest and deepest, enough for β_2 to matter. The same architectural rule from Section 5 predicts the result: homogeneous parameters tolerate SGD; heterogeneous parameters across depths require per-parameter normalization.

7 Discussion

Two miscalibrations in standard eligibility traces, once corrected, remove the need for Jacobian propagation in online recurrent learning. What looked like a temporal credit assignment problem was a gradient scaling problem. The hidden state carries temporal information through the forward pass. The immediate derivative, computed through that state, points in a useful direction for adaptation. The missing piece was gradient scale normalization, not a better Jacobian approximation.

This connects to a structural property of recurrent networks identified in prior work [Shalev Merin, 2026]. The parameter Jacobian of trained RNNs is near-isotropic: its singular values are approximately uniform, with condition numbers between 2.6 and 6.5 at $n = 64$ and scaling as $n^{0.216}$. This isotropy is not learned but inherited from random Gaussian initialization and approximately preserved by training. Because the gradient information is spread roughly evenly across directions in parameter space, any single direction, including the immediate derivative, captures most of the relevant signal. Isotropy explains why the Jacobian term adds so little: when all directions carry similar information, there is no privileged subspace that temporal propagation could reveal.

Why was this not noticed earlier? Three factors reinforced each other. First, nobody measured the actual self-propagation factor. Murray’s RFLO used $\lambda = 0.9$, Bellec’s e-prop used membrane time constants, and 0.95 became convention. Computing $\text{diag}(1 - h_t^2) \cdot \text{diag}(W_{hh})$ is trivial, but nobody did it. Second, Adam did not exist until 2014 [Kingma and Ba, 2015]. The RTRL literature began in 1989. For 25 years, everyone used SGD, and SGD genuinely cannot do online adaptation with immediate-only gradients (Table 1). The conclusion “you need

temporal propagation” was correct for SGD. The field did not revisit it after per-parameter normalization became standard. Third, these errors reinforced each other: if you believe temporal propagation is essential, you will not examine why immediate-only plus SGD fails. When immediate-only plus SGD does fail, you conclude temporal propagation is essential. Nobody tried the combination that breaks the cycle: immediate-only plus Adam.

These findings have clear limits. First, all from-scratch experiments use single-layer networks. In two-layer RNNs, per-layer Jacobians remain isotropic (condition numbers 1.7 and 2.5), but the cross-layer Jacobian is highly anisotropic (condition number 3773). Sparse or immediate gradients within each layer are accurate, but credit assignment from the output layer back through the input layer’s recurrence hits a structural bottleneck. Extending the β_2 finding to deep recurrent networks is an open problem. Second, the tasks tested involve temporal dependencies up to 50 steps. Our claim is about gradient computation, not about long-range credit assignment. If the hidden state does not retain information from step $t - k$ due to vanishing gradients, no gradient method recovers it. Longer-range credit requires architectural solutions such as attention, gating, or structured state spaces, not better gradient approximations. Third, direct online updates to pretrained foundation models produce near-zero adaptation regardless of optimizer. The β_2 finding applies to pretrained models only through parameter-efficient adapters like LoRA, where the adapter’s smaller parameter count allows individual updates to have meaningful magnitude. This has been confirmed from 124M to 7B parameters (Table 5). Fourth, at $n = 256$ and above, recovery percentage shows high variance ($\pm 64\%$) driven by instability in the full RTRL reference rather than in the method itself. Absolute post-shift MSE is more stable across seeds at these scales.

Open questions remain. Deep recurrent networks require addressing the cross-layer anisotropy bottleneck. Whether immediate derivatives remain sufficient under non-gradient learning rules (e.g., predictive coding) is untested. The LoRA results at 7B suggest online adaptation of foundation models is feasible, but the practical engineering (update frequency, adapter rank, stability over long streams) has not been explored.

For any single-layer recurrent architecture trained online, the practical recommendation is: set trace decay to zero and use Adam or RMSprop. This matches or exceeds full RTRL at a fraction of the cost and without any Jacobian computation. For pretrained models, LoRA with Adam achieves online domain adaptation that SGD cannot.

References

Ekin Akyürek, Mehul Damani, Linlu Lin, Sai Vemprala, Dale Schuurmans, and Ashish Kapoor. In-place test-time training for language models. In *ICLR*, 2026.

Guillaume Bellec, Franz Scherr, Anand Subramoney, Elias Hajek, Darjan Salaj,

- Robert Legenstein, and Wolfgang Maass. A solution to the learning dilemma for recurrent networks of spiking neurons. *Nature Communications*, 11(1): 3625, 2020.
- Frederik Benzing, Marcelo Matheus Gauy, Asier Mujika, Anders Martinsson, and Angelika Steger. Optimal Kronecker-sum approximation of real time recurrent learning. *arXiv preprint arXiv:1902.03993*, 2019.
- Heitor M Gomes, Albert Bifet, Jesse Read, Jean Paul Barddal, Fabrício Enembreck, Bernhard Pfharinger, Geoff Holmes, and Talel Abdesslem. Adaptive random forests for evolving data stream classification. *Machine Learning*, 106(9):1469–1495, 2017.
- Danijar Hafner, Jurgis Pasukonis, Jimmy Ba, and Timothy Lillicrap. Mastering diverse domains through world models. *Nature*, 625:118–126, 2024.
- Kazuki Irie, Róbert Csordás, and Jürgen Schmidhuber. Exploring the promise and limits of real-time recurrent learning. *arXiv preprint arXiv:2305.19044*, 2024.
- Diederik P Kingma and Jimmy Ba. Adam: A method for stochastic optimization. *arXiv preprint arXiv:1412.6980*, 2015.
- Éloi Maes, Quentin Le Lidec, Damien Scieur, Yann LeCun, and Randall Balestriero. Learning world models with large language model backbones. *arXiv preprint arXiv:2603.19312*, 2026.
- Owen Marschall, Kyunghyun Cho, and Cristina Savin. A unified framework of online learning algorithms for training recurrent neural networks. *Journal of Machine Learning Research*, 21(135):1–34, 2020.
- Jacob Menick, Jack Rae, and Simon Osindero. A practical sparse approximation for real time recurrent learning. *arXiv preprint arXiv:2104.09750*, 2021.
- Jacob Montiel, Max Halford, Saulo Martiello Mastelini, Geoffrey Bolmier, Raphael Sourber, Robin Vaysse, Adil Zouitine, Heitor Murilo Papadopoulos, et al. River: machine learning for streaming data in Python. *Journal of Machine Learning Research*, 22(110):1–8, 2021.
- James M Murray. Local online learning in recurrent networks with random feedback. *eLife*, 8:e43299, 2019.
- Joseph E O’Doherty, Mariana M B Cardoso, Joseph G Makin, and Philip N Sabes. Nonhuman primate reaching with multichannel sensorimotor cortex electrophysiology. *Zenodo*, 2017. DOI: 10.5281/zenodo.3854034.
- Aur Shalev Merin. Random sparse Jacobian transport in recurrent networks. *arXiv preprint arXiv:2603.15195*, 2026.

- Yu Sun, Xinhao Li, Karan Dalal, Jiarui Xu, Arjun Vikram, Genghan Zhang, Yann Dubois, Xinlei Chen, Xiaolong Wang, Sanmi Kumbhar, et al. Learning to (learn at test time): RNNs with expressive hidden states. In *NeurIPS*, 2024.
- Corentin Tallec and Yann Ollivier. Unbiased online recurrent optimization. *arXiv preprint arXiv:1702.05043*, 2017.
- Dequan Wang, Evan Shelhamer, Shaoteng Liu, Bruno Olshausen, and Trevor Darrell. Tent: Fully test-time adaptation by entropy minimization. In *ICLR*, 2021.
- Ronald J Williams and David Zipser. A learning algorithm for continually running fully recurrent neural networks. *Neural Computation*, 1(2):270–280, 1989.
- Nicolas Zucchet, Simon Schug, Johannes von Oswald, Dominic Zhao, and João Sacramento. Online learning of long-range dependencies. *Advances in Neural Information Processing Systems*, 2023.